Basic properties of a three-dimensional spring-block model with long-range stress transfer

Florian Jansen*
Department of Geodynamics, University of Bonn, D-53115 Bonn, Germany

Stefan Hergarten
Institute of Geosciences, University of Graz, AT-8010 Graz, Austria
(Received 5 October 2005; published 22 February 2006)

Spring-block models have been very useful for understanding slip complexity of earthquakes. So far, however, they have been restricted to one or two dimensions or simple nearest-neighbor stress transfer. Here, we set up a three-dimensional spring-block model with long-range stress transfer and, in a second step, implement several simplifications to realize a considerable gain in computational efficiency. Qualitatively, the two versions do not differ and we use the fast version to investigate basic properties of the model and to compare to the Olami Feder Christensen (OFC) model. The spatial distribution of hypocenters is found to be scale free. At the end of a simulation of 10^7 events, it takes a value of $D_2 \approx 1.8 \pm 0.1$. At this point, however, the spatial slip organization is not stationary yet and the fractal dimension still grows slightly. This does not affect respective frequency size statistics, though, which exhibit a clear power law with a characteristic cutoff that depends on the grid size. The statistics appear smoother than in the OFC model and lack the kink between events of size 1 and 2. In addition, strong periodicities of large events as in the OFC model do not occur in our model. In stark contrast to the OFC model, results remain the same if periodic boundaries are used. Another significant difference is the stableness of results against imposed disorder. Contrary to the OFC model, results do not change if threshold values are randomly distributed in an interval of ±10% around the mean value. Concluding, the model that we propose shares the main properties of the OFC model, but outreaches the latter in being stable in a larger set of configurations.

DOI: 10.1103/PhysRevE.73.026124 PACS number(s): 89.75.Da, 91.30.Bi, 89.75.Fb, 05.45.Ra

I. INTRODUCTION

Natural seismicity results from numerous processes acting on a broad spectrum of scales. For example, earthquake nucleation takes place on a local scale, whereas stress transfer on a given fault, and the interaction between different faults occur over much larger scales. A comprehensive model of all processes that govern seismicity does not yet exist, but even if all processes were known in detail, computational constraints would still be a limiting factor. As a consequence, seismological modeling largely focuses on a subset of seismic properties and scales, such as the ubiquitous observation of scale-invariance in frequency size (FS) statistics of earthquakes.

Scale-invariance has been qualitatively reproduced by a particularly simple but rich class of approaches known as spring-block models. The physical basis for these models is the slow accumulation of stress through tectonic loading coupled to the sudden relief of stress when a failure condition is met. The first model of this type consisted of a one-dimensional chain of masses governed by stick-slip motion under the applied rules [1]. In this model, an earthquake corresponds to a chain reaction of sliding blocks on an existing surface, which is governed by the interplay between friction and elastic interactions. Later works used two-dimensional cellular automata [2–4] and related the dynamics of their systems to the concept of *self-organized criticality* [5–7]. These models provided a mechanism that led to Gutenberg-Richter (GR) like FS statistics without any tuning of the system. The simple nearest-neighbor rules of the Olami-Feder-Christensen (OFC) model, as one of their most studied members, produce an internal complexity that even accounts for temporal clustering of events consistent with Omori's law for aftershocks at a qualitative level [4,8]. In addition to analyses of the FS statistics, Ito and Matsuzaki included investigation of the fractal distribution of earthquake epicenters generated by their model [3]. While obtaining results that are in agreement with empirical values, they point out that a three-dimensional model would be more realistic for simulating earthquakes as anisotropy could be incorporated. Likewise, Peixoto and Prado studied statistics of epicenters in the OFC model in two and three dimensions [9]. In the case of the three-dimensional OFC model, however, the applied rule for equal stress transfer to all nearest neighbors is not justified in terms of the stress redistribution around a shear crack.

Regarding underlying physics and the stress transfer in elastic solids, a shortcoming of the mentioned models is the limitation of stress transfer to nearest neighbors. Weatherley *et al.* analyzed the dependence of FS statistics in a two-dimensional spring-block model on the mode of stress transfer and found that for short-range stress transfer, they obtain GR type statistics and for long-range stress transfer statistics that agree with the characteristic earthquake distribution [10]. This result, however, is not unique as is shown by the work of Chen *et al.*, who modeled crack propagation in two-dimensional and three-dimensional grids [11]. Local breakdown of elastic forces leads to long-range redistribution of

*Electronic address: jansen@geo.uni-bonn.de

stress, but, contrary to Weatherley, the model generates GR like statistics, with a b value of $b \approx 0.4$ in two and $b \approx 0.6$ in three dimensions, respectively.

While the former models all describe slip events on a given surface and associate the size of an earthquake with the amount of slipped blocks, the model of Chen *et al.* describes the propagation of a crack in a brittle medium and relates the successive breaking of springs to earthquakes. Consequently, earthquakes are not restricted to prescribed fault planes. The same concept is followed by Sahimi *et al.* and Arbabi *et al.* who investigated mechanical breakdown of disordered solids [12,13]. They use three-dimensional grids of sites that are connected by springs and governed by elastic interactions up to a threshold value. Once a spring reaches its threshold value, it is broken irreversibly. Elastic properties are varied in different ways, which are analyzed with regards to the respective mode of macroscopic failure. This model was used to suggest that a percolation process accounts for both the geometry of fault patterns and the spatial distribution of earthquakes [14].

Here, we set up a continously driven, nonconservative spring-block model in three dimensions. The model simulates earthquake sequences of a finite fault zone where slip is not confined to a predefined plane. We calculate the stress redistribution through a Green's function of a slipping block, which results in long-range stress transfer including both regions of stress increase and of stress decrease. In a second step, we implement several simplifications to realize a considerable gain in computational efficiency.

II. MODEL DESCRIPTION

We analyze the response of a three-dimensional brittle material subjected to continuous shearing under vertical constraint. The material behaves elastically to a certain threshold value, after which the material fails via slip within the body that perturbs the local and far-field stress field. The stress redistribution may lead to a propagation of the failure and cause extended areas to fail successively.

As in most earthquake models, the timescales of tectonic loading and individual earthquakes are decoupled. That is, the system is loaded via shear until failure begins on one cell, and then shearing is halted during the subsequent failure sequence. Our model does not include the dynamics associated with a failure, but restricts itself to the determination of the stress field before and after failure. In regard to failed elements, stress drops to zero and those elements reenter the elastic regime (more details given below).

We describe two versions of the model. In the first version, called the basic model, we incorporate an exact solution for calculation of the stress field associated with failure. However, the exact solution is computationally cumbersome, so we also explore a much faster algorithm that makes several simplifications.

A. Basic model

The model consists of a three-dimensional grid of $N \times N \times N$ blocks, each of which is connected by springs to its six nearest neighbors (Fig. 1). Shearing of the grid is constrained to one direction and only the forces on vertical springs are considered. The springs' stiffness is equally set to one and each spring is given a uniform maximum force F_{crit} that it can support. On reaching this threshold, a spring breaks and is replaced by a new spring with zero force after the grid has been updated.

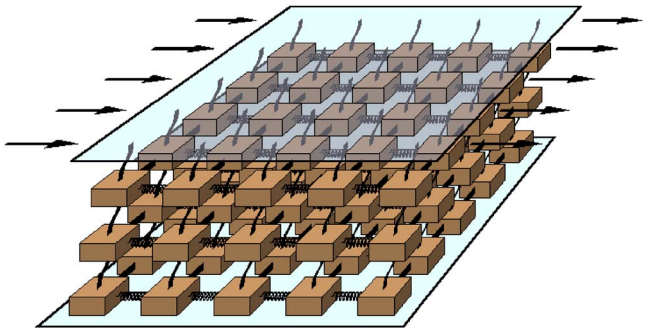

FIG. 1. (Color online) Setup of a three-dimensional spring-block model. Shearing is in one direction only and vertical displacements are not allowed.

As we do not look at the elastodynamics of the earthquake process, we can use the constraint that all blocks are at rest after reaching their final position. Therefore the sum of all elastic forces acting on a block must be zero:

$$\sum_{j=1}^{6} u_j' - u_i' = 0. \tag{1}$$

In this equation, $u_j' - u_i'$ is the relative displacement of blocks i and j that occurred since the spring that connects the two blocks was inserted into the grid. The corresponding set of N^3 linear equations is solved by a *conjugate gradient method* [15], which is a semi-iterative scheme that arrives at the exact solution after N^3 steps. Since the effort per step is proportional to N^3, the total numerical effort required for solving the set of linear equations is of the order of N^6. By losing bonds in the case of breaking of one or more springs, the set of linear equations transforms into a new one, which determines the displacements after failure. The associated redistribution of stress may cause further springs to break, requiring the next recalculation. Each recalculation is regarded as one relaxation cycle and after each relaxation cycle, all broken springs are replaced by new ones with zero force. The whole series of relaxation cycles until no further breakings occur is termed an event.

At start of a simulation, all blocks are assigned a random slip history accompanied by the corresponding stress field. Successively, the grid is always sheared to the point where the next spring reaches its threshold value and halted at that point. Since any shearing results in equal stress increase on all springs as long as no springs break, this point can easily be calculated and the displacements and corresponding stresses be updated respectively. Following, the sequence of relaxation cycles is calculated until the event ceases and the grid is sheared to the next breaking condition. By applying this procedure we get a continously driven model.

The total stress redistribution associated with one relaxation cycle sums up to a stress drop, which makes the model inherently nonconservative and causes events eventually to stop. The actual amount of this stress drop depends on the forces that acted on the failed springs before breaking and is given, in the case of one breaking spring, as

$$\sum_{i=1}^{N^3} \Delta\sigma_i \approx -1.5 \times F_{fail}, \tag{2}$$

where the relationship is exact in the limit of inifinte grid size.

B. Fast model

The time needed for recalculation of the stress field after breaking of springs scales with the grid size N as N^6 in the basic model. Simulation of, e.g., 10 000 events for a grid of size $N=50$ takes several weeks. To provide for larger statistics, we aim at an algorithm that does not need to resolve the whole system of equations after each breaking. An ideal algorithm would make use of a *relaxation rule* as used by the OFC model, meaning that for each redistribution of stress, a prescribed set of rules is applied. Thus no set of equations has to be solved and the respective numerical effort becomes independent of grid size. Based on the work we have done, however, it appears that there does not exist a relaxation rule for the three-dimensional model that keeps the model's behavior. Nevertheless, we could reduce numerical effort significantly by using several simplifications.

In a first step, we make use of discretized Green's functions, a common tool in continuum mechanics. For a given grid size, we can calculate all finite Green's functions by means of the *conjugate gradient method* and use them in later simulations to calculate the stress redistribution after failure. Let G^i be the Green's function for failure of block i. To update the stress of block j, the respective value of the Green's function, G^i_j, has to be multiplied with the force which acted on the spring i before it broke. The benefit of this step is to reduce numerical effort from N^6 to N^3.

However, there is one drawback of this procedure, which leads to the first of the following succession of simplifications:

(i) Only one spring breaks at a time:

The Green's function that is to be used depends on the spring or subset of springs that broke. Since we do not know beforehand which springs are going to break in a simulation, we would have to consider all possible subsets of the grid, which amounts to $\Sigma_{m=1}^{N}\binom{N^3}{m}$ different Green's functions. Calculating all these finite Green's functions would be equally cumbersome. Additionally, storing all respective values during a simulation would quickly exceed all available working memory. Therefore we make the assumption that only one spring breaks at a time, which keeps the amount of necessary Green's functions to N.

This simplification means that an incidence of m breaking springs is resolved into a sequence of m single breakings. Simulations showed that the general behavior of the model does not change by applying this step.

(ii) Boundary effects are neglected:

We further reduce the amount of Green's functions to be stored by using the same one for each breaking spring, namely the one derived for failure of the spring in the center of the grid. We thus reduce demanded storage capacity during simulation from N^6 to N^3. Again, impact on the simulations turned out to be minor. Naturally, the influence grows bigger as the grid gets smaller, but we found no significant difference in the results for grids bigger than $N=64$.

(iii) Stress transfer is confined to a limited region:

As the influence on the stress field falls as $1/r^3$ with distance r to the failed spring, we take another step which brings us closer to a *relaxation rule*. After breaking of a spring, we do not recalculate the stress field of the whole grid, but only for blocks belonging to a cuboid centered around the broken spring. The cuboid will be termed the *transfer region* (TR). We conjecture that the model's main features are not determined by stress changes which fall below a certain fraction of the main impact occurring in the near field.

Depending on the size of the transfer region we get a compromise between accuracy, relative to the basic model, and efficiency of the algorithm. This last step reduces numerical effort from N^3 to N^0.

The biggest gain in efficiency comes with step iii if the transfer region is limited to a small cuboid. Because of the dipole like pattern of stress redistribution in the basic model, we choose the horizontal extension of the TR twice as large as the vertical. Thus we are roughly guided by isolines of the stress change in setting the boundaries of the TR. Let the indices of a failed block be ijk. We will then refer to a TR that includes blocks with indices $i,j \in (i-h,j-h;i+h,j+h)$ and $k \in (k-v;k+v)$ as of size v/h. Considering a grid of size $N=128$, chosing a transfer region of size 3/6, for example, results in a numerical effort proportional to $(2\times3+1)(2\times6+1)^2=1183$ as compared to $128^3=2\,097\,152$ in the basic model.

However, the assumption that minor stress changes do not influence the model's behavior does not hold if a systematic deviation is summed up over long event sequences. As was mentioned at the end of Sec. II A, each relaxation cycle leads to an accumulated stress change, the amount of which is given by Eq. (2). Due to the linearity and boundary conditions of the system of equations, this stress drop is evenly distributed over all N layers, with the value for each layer being

$$\sum_{i_l} \Delta\sigma_{i_l} \approx -1.5 \times F_{fail}/(N-1). \tag{3}$$

What turns out to be crucial is that this property is only reached if we sum over all blocks belonging to a layer. Inside given subsets, the sum of stress change differs sligthly from layer to layer. These differences get bigger the smaller the subsets get. Hence confining stress transfer to a limited TR means that for each layer, we get a deviation of the accumulated stress change from its must value according to Eq. (3). During a respective simulation, this leads to a systematic deviation which accumulates increasing mismatches in mean stress between adjacent layers. These mismatches are recur-

rently reduced in excessively big events. Since this feature neither occurs in the basic model nor in steps ii and iii, it appears clear that it is caused by the disregard of uniform stress drop per layer.

To avoid this problem, we searched a way to adhere to the uniform stress drop, while still keeping numerical effort proportional to N^0. The latter implies that upon failure of a spring we do not want to treat the blocks of all grid layers individually. Thus ensuring a uniform stress drop over all layers can only be done by relaxing each block in the grid by the same amount, which can numerically be solved by introducing a respective global variable. This procedure, however, implies that the accumulated stress drop inside the TR has to be zero. To meet this last condition, we modify the stress field inside the TR a second time after we have redistributed stress according to the Green's function.

Details of this modification are given in the following.

Modification of stress transfer inside the TR

Readjusting the accumulated stress change inside the TR can be done in several different ways, e.g., by shifting the stress of all blocks by a constant value. Surprisingly, the different schemes did not significantly change simulation results. To maintain the relative "topography" of stress change of the original Green's function as well as possible, we chose the following scheme for our results section.

The modifications follow two principles: (i) No stress change is allowed to alter its algebraic sign; and (ii) the blocks' relative order concerning their absolute value of stress change shall be kept.

The following list summarizes the numerical steps, with steps (a) and (b) being performed individually for each layer of the TR and step (c) only once at the end of each relaxation cycle:

(a) While changing stress according to the Green's function, keep track of the accumulated stress change and the accumulated absolute value of stress change,

$$\sum_{i_{l,TR}} \Delta\sigma_{i_{l,TR}} \text{ and } \sum_{i_{l,TR}} \Delta|\sigma_{i_{l,TR}}|.$$

(b) Subtract from each block inside the transfer region a fraction of the accumulated stress change, which is weighted by the absolute value of stress change that the block received in step (a). The net stress change for block i in layer l inside the TR after steps (a) and (b) thus becomes

$$\Delta\sigma'_{i_{l,TR}} = \Delta\sigma_{i_{l,TR}} - \frac{\Delta|\sigma_{i_{l,TR}}|}{\sum_{i_{l,TR}} \Delta|\sigma_{i_{l,TR}}|} \times \sum_{i_{l,TR}} \Delta\sigma_{i_{l,TR}}. \quad (4)$$

This results in the new accumulated stress change being zero.

(c) Add the (negative) value $\Sigma_{i_l}\Delta\sigma_{i_l}/N^2$ to every block in the grid, which after step (b) results in the correct value $\Delta\sigma_{i_l}$ [as given by Eq. (3)] for each layer l. As the stress change in this step is the same for every block, this step can be performed by introducing a respective global variable.

By applying this procedure, the property of uniform stress change is maintained while still keeping numerical effort proportional to the size of the transfer region. However, the smaller the TR becomes, the bigger the deviation gets that has to be accounted for in the modification of the stress transfer. As we will see in Sec. III, this results in a tendency to a smaller b value and an excess of big events.

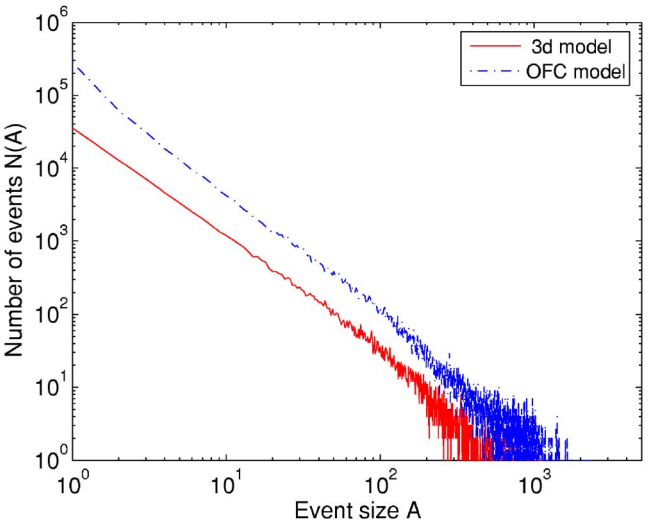

FIG. 2. (Color online) Comparison of FS statistics for three-dimensional and OFC model (grid size $N=65$, 7×10^4 events for three dimensional model and 7×10^5 events for OFC model, respectively).

III. RESULTS

We analyzed FS statistics and the spatial distribution of hypocenters in terms of scale invariance. Furthermore, we chose FS statistics as a criterion both to validate the applicability of the fast model and to compare with the OFC model.

We obtained FS statistics for 90 000 events on a simulation of the basic model on a grid of size $65\times65\times65$ (the simulation took about 6 months, which compares to about 10 min if run with the fast model and a TR size of 3/6). The FS statistics exhibit a clear power law over two magnitudes with a b value of $b\approx0.48$. Chen *et al.* obtained a value of $b\approx0.6$ when simulating 10 000 events on a grid of size $20\times20\times20$. The FS statistics of Chen *et al.* are not as smooth as in our model, presumably because of the small grid they use and the rather short simulation. In comparison with the OFC model ($\alpha=0.2$ which corresponds to a level of conservation of 80%), our results show a power law which is somewhat smoother and lacks the characteristic kink of the OFC model that occurs at the transition from events of size $s=1$ to $s=2$ (Fig. 2).

We repeated the simulation described above using the fast model with two different TR sizes and compared the results to that of the basic model (Fig. 3). Our aim was to determine how the simplifications of the fast model affect the FS statistics and to assess the influence of the TR size. The results show that, when using large transfer regions, the FS statistics differ only slightly from those of the basic model. However, reducing the size of the TR has two effects: (i) the b value of the FS statistics becomes slightly smaller; and (ii) there is an excess of big events.

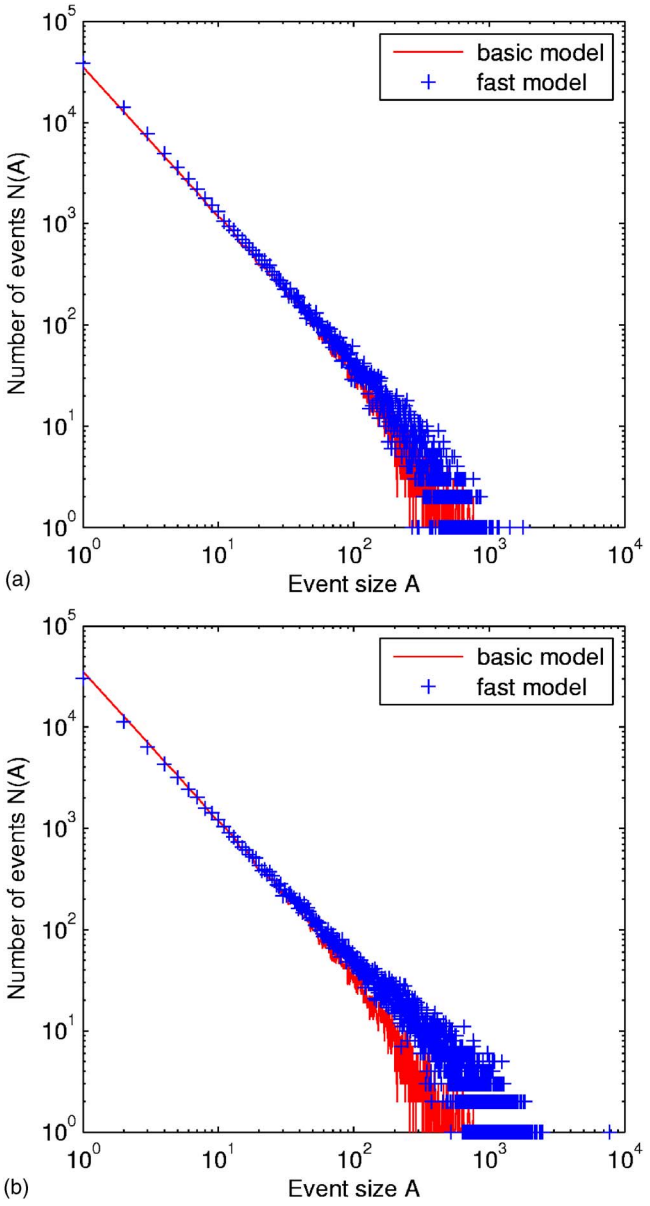

FIG. 3. (Color online) Comparison of FS statistics as calculated by the basic and the fast algorithm (grid size $N=65$, 7×10^4 events); TR size for the fast algorithm is 16/32 for (a) and 3/6 for (b). For definiton of TR see Sec. II B.

Since we wanted to investigate the qualitative behavior of the three-dimensional model rather than to give precise values of scaling exponents, we used the fast model from now on, which allows for much larger statistics. The statistics that we generated with the basic model, however, indicate that the following results are also characteristic of the basic model.

Calculations for five different grid sizes ranging from $N=17$ to $N=257$ all show a clear power law with a relatively constant b value. The results also exhibit the typical exponential cutoff that depends on the grid size (Fig. 4).

To estimate the fractal dimension of the spatial distribution of hypocenters, we used the two-point correlation dimension D_2, as did Ito and Matsuzaki [3]. The correlation dimension D_2 is considered to be close to the fractal dimension D. Using a sequence of N events, we first calculate the correlation integral $C'(r)$:

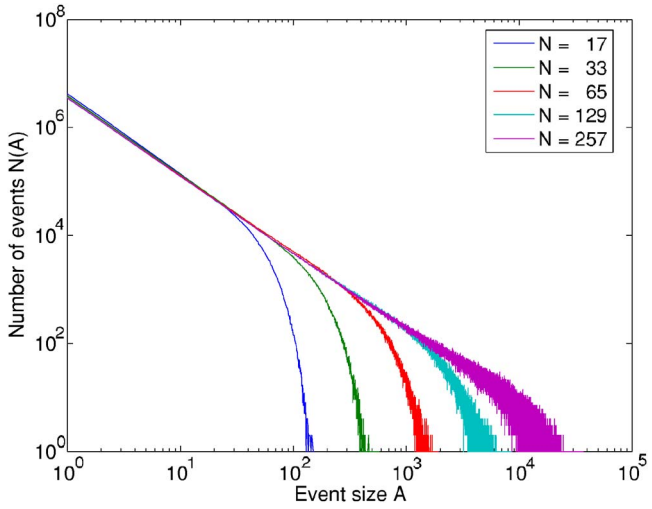

FIG. 4. (Color online) FS statistics for five different grid sizes (increasing rightwards) as indicated in the plot's legend (each 10^7 events, TR size 3/6).

$$C'(r) \equiv \frac{1}{N^2}\sum_{i=1}^{N}\sum_{j=i+1}^{N} H(r-|X_i-X_j|), \tag{5}$$

where $H(x)$ is the Heaviside function and $|X_i-X_j|$ the distance between hypocenters of events i and j. In a second step, we evaluate D_2 by using the fact that for a certain range of distances r, the correlation integral behaves as

$$C'(r) \propto r^{D_2}. \tag{6}$$

This range basically excludes very small and large distances for reasons of grid discreteness and finiteness, respectively. In between, however, we get a smooth power law, from which we estimate the fractal dimension according to Eq. (6). Considering N, we chose a value of 2000, meaning that for a simulation consisting of 10^7 events we obtain 5000 representative values for the fractal dimension. We found three main properties [Fig. 5(a)]:

(i) At start of the simulation, the fractal dimension D_2 is rather small and grows as the simulation proceeds.

(ii) Deviation of D_2 grows with ongoing simulation.

(iii) The value of D_2 depends on the size of the transfer region.

We performed a similar analysis for the OFC model, where D_2 was on average constant throughout the simluation, but showed a deviation that exceeded the one of the three-dimensional model. Comparison with the results of Ito and Matsuzaki is not very meaningful, because they calculated only about 12 values for D_2 at the start of the simulation. In that range, our simulation does not show a large deviation.

The third point stems from the internal organization of slip concentration. Simulations start with slip primarily limited to a horizontal plane. As the simulation proceeds, the vertical extent of slip increases and hypocenter locations fill a larger part of the volume. As a measure of this evolution, we monitored the amount of layers involved in one event,

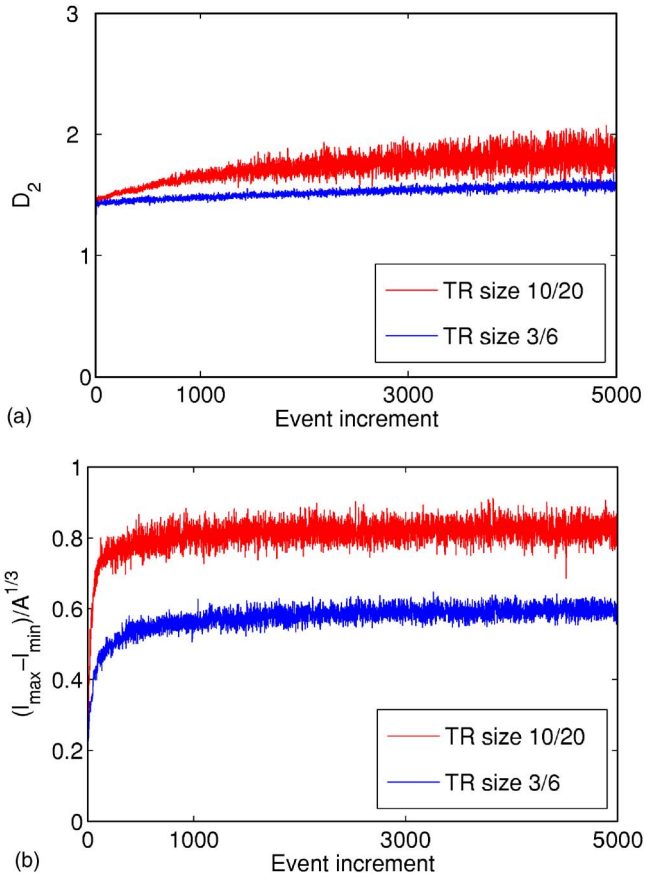

FIG. 5. (Color online) Evolution of fractal dimension D_2 (a) and normalized vertical extent of events (b) for two different TR sizes (grid size N=65, 10^7 events).

devided by the third root of the event size [Fig. 5(b)]. This value should be close to 1 for a totally isotropic model. As the simulation proceeds, events get more and more "spherical" which corresponds to the fact that more and more layers become available for slip. This evolution takes place faster for larger transfer regions because the stress redistribution affects blocks at longer ranges. However, this difference is only transient as we found by performing the same monitoring after skipping 10^9 events.

At the end of the simulation, the fractal dimension takes a value of $D_2 \approx 1.8 \pm 0.1$, which compares to $D_2 \approx 1.3 \pm 0.1$ for the two-dimensional OFC model. However, the value still grows as the simulation proceeds and convergence towards a limit of about 2 cannot be precluded on the basis of the present simulations.

Here, we compare some basic properties of our model with those of the two-dimensional OFC model.

The evolving FS statistics of the three-dimensional model appear smoother than those found in the OFC model. We quantify this difference by choosing a measure of smoothness termed Δ that is based on the standard deviation of event size numbers. Assuming that event size numbers $N(A)$ for a given event size A are Gaussian distributed with a mean value of $\bar{N}(A)$ and a standard deviation of $\sqrt{N(A)}$ for big enough event numbers N (in our case $N > 1000$), we define the following measure of deviation:

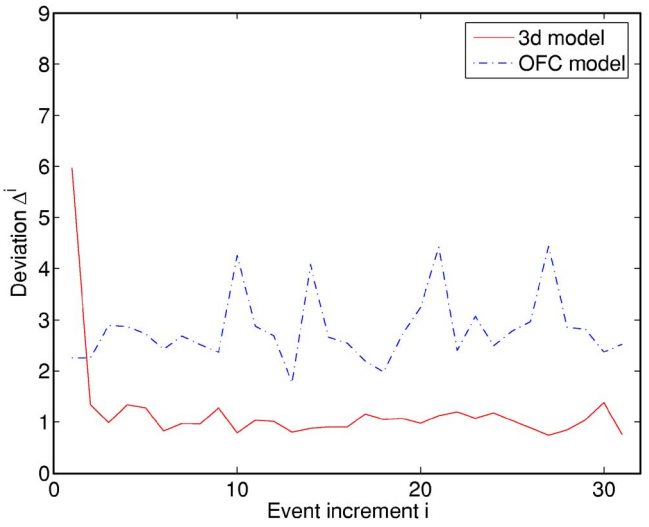

FIG. 6. (Color online) Comparison of standardized deviation of three-dimensional [solid (red) line] and OFC model [dashed (blue) line]. For definition of the deviation Δ^i refer to text [Eq. (7)].

$$\Delta^i = \frac{1}{A_{max}} \sum_{A=1}^{A_{max}} \left(\frac{N^i(A) - \bar{N}(A)}{\sqrt{N^i(A)}} \right)^2 \tag{7}$$

with

$$\bar{N}(A) = \frac{1}{i_{max}} \sum_{i=1}^{i_{max}} N^i(A).$$

The index i refers to all events from the interval $[(i-1)10^7; i10^7)$ and is termed the *event increment*. Thus each value Δ^i is a representative value for a subset of 10^7 events of the running simulation. Using this measure, a simulation of 3×10^8 (i_{max}=30) events supports the impression that FS statistics tend to be smoother in the three-dimensional model (Fig. 6).

Analyses of time series generated by the OFC model have indicated a complex behavior. While events are clustered on the short time scale, large events tend to occur rather periodically with a recurrence interval that depends on the level of conservation. Event sequences spanning an interval of ten model units (corresponding to about 5×10^6 events) clearly show these periodicities [16]. In contrast, respective simulations of the three-dimensional model do not share this property (Fig. 7). This supports the assumption that events occur uncorrelated in the three-dimensional model, which is in line with the results of the previous subsection (Fig. 6). However, this conclusion basically holds for long time series as Fig. 6 samples values for sequences of 10^7 events each. Moreover, temporal clustering is not sure to be detected by mere visual impression. In the case of the OFC model, sequences of fore- and aftershocks had not been described until ten years after the publication of the original paper on the model [8]. Therefore it would be valuable to further analyze the three-dimensional model for temporal clustering on the short time scale.

Two drawbacks of the OFC model are its sensitivity to its boundary condition and to imposed disorder. We analyzed

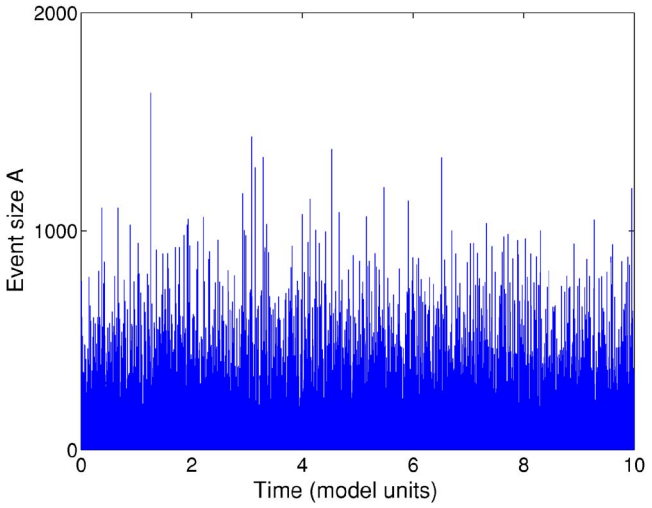

FIG. 7. (Color online) Time series of an event sequence produced by the fast algorithm with a TR of size 3/6. The time span of one model unit corresponds to the time it takes to load a spring of zero force up to its threshold value. This holds for both the OFC model and the three-dimensional model.

the three-dimensional model when run with horizontally periodic boundary conditions and with a random spreading of the critical value that a spring can support, respectively. In the latter case, we draw the threshold values from a uniform distribution in the interval [0.9; 1.1]. We performed the same simulations with a corresponding version of the OFC model for comparison. Surprisingly and contrary to the OFC model, neither horizontally periodic boundaries nor imposed disorder of the order of 10% of the threshold value influence the obtained FS statistics in the three-dimensional model (Figs. 8 and 9).

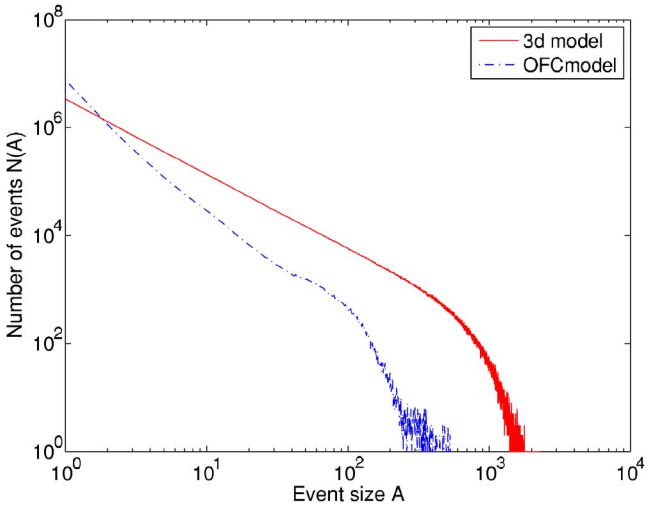

FIG. 8. (Color online) Comparison of FS statistics for three-dimensional and OFC model with periodic boundaries (grid size $N=65$, 10^7 events).

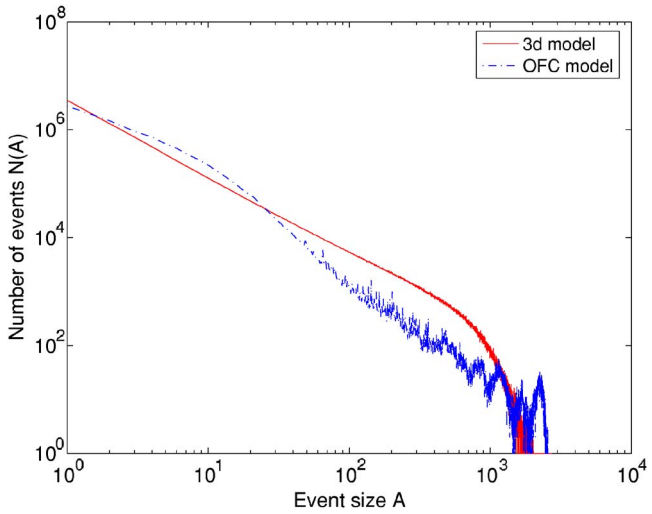

FIG. 9. (Color online) Comparison of FS statistics for three-dimensional and OFC model with randomly distributed threshold values (grid size $N=65$, 10^7 events).

IV. CONCLUSIONS

We propose a model for simulation of a fault, where slip is not confined to a plane, but may occur in a region of finite thickness. To this end, we have set up a continously driven, nonconservative spring-block model in three dimensions with long-range stress transfer. In a second step, we have implemented several simplifications to realize a considerable gain in computational efficiency. Qualitatively, the two versions do not differ and we have used the fast version to investigate extended statistics in terms of scale invariance and to compare to the well known results of the two-dimensional OFC model.

The spatial distribution of hypocenters is found to be scale free. Based on a sequence of 10^7 events, we estimate a fractal dimension of $D_2 \approx 1.8 \pm 0.1$. However, this value still grows slightly, meaning that spatial organization of slip has not reached stationarity yet.

Analogous to the OFC model, obtained FS statistics exhibit a clear power law over several magnitudes with a characteristic cutoff that depends on the grid size. FS statistics are somewhat smoother than in the OFC model and lack the characteristic kink at the transition from events of size $s=1$ to $s=2$. The strong periodicity of large events as known from the OFC model has not been detected in event sequences of the three-dimensional model. This supports the assumption that events tend to occur uncorrelated on long timescales.

Observed FS statistics remain the same if periodic boundaries are used, which is in stark contrast to the OFC model. Thus the often cited suggestion that the emerging state of criticality in the OFC model has its cause in the specific boundary condition cannot hold in the three-dimensional model. Another striking difference is the stableness of results against imposed disorder. Contrary to the OFC model, results do not change if threshold values are not set uniform but randomly distributed in an interval of ±10% around the mean value. This is a remarkable advantage over the OFC model regarding its applicability to natural seismicity.

We conclude that while the three-dimensional model that we propose shares the OFC model's essential properties it outreaches the latter one in being stable in a larger set of configurations. To find out what restrictions of the OFC model, as compared to our model, are responsible for its shortcomings, dedicated tests would have to be performed. This would certainly add to the understanding of the OFC model and of spring-block models in general.

ACKNOWLEDGMENTS

This work has been supported by the DFG (Deutsche Forschungsgemeinschaft), in the context of the post graduate programme 437 at the University of Bonn. We thank Stephen Miller for useful discussions and improvements to the manuscript.

[1] R. Burridge and L. Knopoff, Bull. Seismol. Soc. Am. **57**, 341 (1967).
[2] P. Bak and C. Tang, J. Geophys. Res. **94**, 15 635 (1989).
[3] K. Ito and M. Matsuzaki, J. Geophys. Res. **95**, 6853 (1990).
[4] Z. Olami, Hans Jacob S. Feder, and K. Christensen, Phys. Rev. Lett. **68**, 1244 (1992).
[5] P. Bak, C. Tang, and K. Wiesenfeld, Phys. Rev. Lett. **59**, 381 (1987).
[6] P. Bak, *How Nature Works—The Science of Self-Organized Criticality* (Copernicus, Springer, Berlin, New York, 1996).
[7] H. J. Jensen, *Self-organized Criticality—Emergent Complex Behaviour in Physical and Biological Systems*, Vol. 10 of Lecture Notes in Physics (Cambridge University Press, Cambridge, England, 1998).
[8] S. Hergarten and H. J. Neugebauer, Phys. Rev. Lett. **88**, 238501 (2002).
[9] T. P. Peixoto and C. P. C. Prado, Physica A **342**, 171 (2004).
[10] D. Weatherley, P. Mora, and M. Xia, Pure Appl. Geophys. **159**, 2469 (2002).
[11] K. Chen, P. Bak, and S. P. Obukhov, Phys. Rev. A **43**, 625 (1991).
[12] M. Sahimi and J. D. Goddard, Phys. Rev. B **33**, R7848 (1986).
[13] S. Arbabi and M. Sahimi, Phys. Rev. B **41**, 772 (1990).
[14] M. Sahimi, M. C. Robertson, and C. G. Sammis, Phys. Rev. Lett. **70**, 2186 (1993).
[15] J. Stoer and R. Bulirsch, *Introduction to Numerical Analysis*, Vol. 12 of Texts in Applied Mathematics (Springer, Berlin, New York, 2002).
[16] S. Hergarten, *Self-Organized Criticality in Earth Systems* (Springer, Berlin, 2002).